Performance analysis of incoherent multi-wavelength OCDMA systems under the impact of four-wave mixing

Ngoc T. Dang and Anh T. Pham*

Graduate Department of Computer and Information Systems, The University of Aizu, Aizu-wakamatsu city, Fukushima 965-8580, Japan
**pham@u-aizu.ac.jp*

Abstract: In this paper, we comprehensively analyze the impact of four wave mixing (FWM) on the performance of incoherent multi-wavelength optical code-division multiple-access (MW-OCDMA) systems. We also consider many other interferences and noises, including multiple access interference, optical beating interference, and receiver noise, in the analysis. From the numerical results, we can find the power ranges of different MW-OCDMA systems, in which the impact of FWM is dominant and consequently results in an increase in the bit-error rate of the systems. We also find that the impact of FWM becomes more severe when the frequency spacing is small and/or dispersion-shifted fiber is used. In addition, we quantitatively discuss the impact of FWM on the number of supportable users and power penalty in the MW-OCDMA systems.

OCIS codes: (060.0060) Fiber optics and optical communications; (060.4230) Multiplexing.

References and links

1. A. Stok and E. H. Sargent, "The role of optical CDMA in access networks," IEEE Commun. Mag. **40**(9), 83–87 (2002).
2. D. Zaccarin, and M. Kavehrad, "An optical CDMA system based on spectral encoding of LED," IEEE Photon. Technol. Lett. **5**(4), 479–482 (1993).
3. L. Tancevski, and I. Andonovic, "Hybrid wavelength hopping/time spreading schemes for use in massive optical networks with increased security," J. Lightwave Technol. **14**(12), 2636–2647 (1996).
4. C.-S. Brès, Y.-K. Huang, I. Glesk, and P. R. Prucnal, "Scalable asynchronous incoherent optical CDMA," J. Opt. Netw. **6**(6), 599–615 (2007).
5. E. D. J. Smith, P. T. Gough, and D. P. Taylor, "Noise limits of optical spectral-encoding CDMA systems," Electron. Lett. **31**(17), 1469–1470 (1995).
6. E. D. J. Smith, R. J. Blaikie, and D. P. Taylor, "Performance enhancement of spectral-amplitude-coding optical CDMA using pulse-position modulation," IEEE Trans. Commun. **46**(9), 1176–1185 (1998).
7. L. Tancevski, and L. A. Rusch, "Impact of the beat noise on the performance of 2-D optical CDMA systems," IEEE Commun. Lett. **4**(8), 264–266 (2000).
8. Z. Wei, H. M. H. Shalaby, and H. Ghafouri-Shiraz, ""Modified quadratic congruence codes for fiber Bragg-grating-based spectral-amplitude-coding optical CDMA systems," IEEE/OSA," J. Lightwave Technol. **19**(9), 1274–1281 (2001).
9. A. Pham, N. Miki, and H. Yashima, "Spectral-amplitude-encoding optical-code-division-multiplexing system with a heterodyne detection receiver for broadband optical multiple-access networks," J. Opt. Netw. **4**(10), 621–631 (2005).
10. A. T. Pham, and H. Yashima, "Performance enhancement of the 2-D wavelength-hopping/time-spreading synchronous OCDM system using a heterodyne detection receiver and PPM signaling," J. Opt. Netw. **6**(6), 789 (2007).
11. T. Ngoc Dang, Anh T. Pham, and Zixue Cheng, "Impact of GVD on the performance of 2-D WH/TS OCDMA systems using heterodyne detection receiver," IEICE Trans. on. Fundamentals E **92-A**, 1182–1191 (2009).
12. C. Zuo, W. Ma, H. Pu, and J. Lin, "The impact of group velocity on frequency-hopping optical code division multiple access system," J. Lightwave Technol. **19**(10), 1416–1419 (2001).
13. G. P. Agrawal, *Fiber-optic communication systems* (A John Wiley and Sons, 2002).
14. N. Shibata, K. Nosu, K. Iwashita, and Y. Azuma, "Transmission limitations due to fiber nonlinearities in optical FDM systems," IEEE J. Sel. Areas Comm. **8**(6), 1068–1077 (1990).
15. K. Inoue, and H. Toba, "Theoretical evaluation of error rate degradation due to fiber four-wave mixing in multichannel FSK heterodyne envelope detection transmission," J. Lightwave Technol. **10**(3), 361–366 (1992).

#120788 - $15.00 USD Received 1 Dec 2009; revised 1 Mar 2010; accepted 22 Apr 2010; published 27 Apr 2010

16. K. Inoue, K. Nakanishi, K. Oda, and H. Toba, "Crosstalk and power penalty due to fiber four-wave mixing in multichannel transmissions," J. Lightwave Technol. **12**(8), 1423–1439 (1994).
17. R. W. Tkach, A. R. Chraplyvy, F. Forghieri, A. H. Gnauck, and R. M. Derosier, "Four-photon mixing and high-speed WDM systems," J. Lightwave Technol. **13**(5), 841–849 (1995).
18. T. Ngoc, Dang and Anh T. Pham, "FWM impairment in multi-wavelength optical code-division multiplexing systems" in *Proc. of the Australasian Telecommunication Networks and Applications Conference*, (2009).
19. T. Ngoc, Dang and Anh T. Pham, "Impact of four-wave mixing on 2-D optical code-division multiplexing systems" in *Proceedings of IEEE Photonics Society Summer Topicals'09*, (Institute of Electrical and Electronics Engineers, New York, 2009), pp. 29–30.
20. A. Grunnet-Jepsen, A. E. Johnson, E. S. Maniloff, T. W. Mossberg, M. J. Munroe, and J. N. Sweetser, "Fiber Bragg grating based spectral encoder/decoder for lightwave CDMA," Electron. Lett. **35**(13), 1096–1097 (1999).
21. J. Magne, D.-P. Wei, S. Ayotte, L. A. Rusch, and S. LaRochelle, "Experimental demonstration of frequency-encoded optical CDMA using superimposed fiber Bragg gratings," in Proceeding of OSA Top. Mtg. on Bragg gratings, photosensitivity, and poling, (Québec, Canada 2003), pp. 1–6.
22. H. Tamai, H. Iwamura, N. Minato, and S. Oshiba, "Experimental study on time-spread/wavelength-hop optical code division multiplexing with group delay compensating en/decoder," IEEE Photon. Technol. Lett. **16**(1), 335–337 (2004).
23. Recommendation G.694.1, *Spectral grids for WDM applications: DWDM frequency grid*, (ITU-T 2002).
24. Recommendation G.652, *Characteristics of a single-mode optical fibre and cable*, (ITU-T 2005).
25. Recommendation G.653, *Characteristics of a dispersion-shifted single-mode optical fibre and cable*, (ITU-T 2006).
26. Recommendation G.655, *Characteristics of a non-zero dispersion-shifted single-mode optical fibre and cable*, (ITU-T 2006).

1. Introduction

Optical communication systems have been playing an important role in telecommunication networks in general and access networks in particular. In order to make use of the vast bandwidth provided by optical fiber, multiple-access techniques have been proposed, such as time-division multiple-access (TDMA), wavelength-division multiple-access (WDMA), and optical code-division multiple-access (OCDMA). In the area of optical access networks, OCDMA has been regarded as a promising candidate thanks to its advantages over conventional techniques. First and the most important one is that OCDMA allows users to access the network asynchronously and simultaneously without strict timing synchronizations and wavelength managements as in the cases of TDMA and WDMA, respectively. In addition, OCDMA network can support a large number of users, which has a soft limit with a graceful degradation of performance with increasing number of users. Finally, OCDMA's ability of offering service differentiation at the physical layer and its inherent security are advantages that no other techniques can provide [1].

In OCDMA systems, transmitted signal can be encoded using either time or frequency domain. The disadvantage of time-domain encoding OCDMA is its spectral inefficiency. Incoherent multi-wavelength OCDMA (MW-OCDMA) is the class of OCDMA technique that uses the spectral amplitudes of carrier signal to encode data hence offers better spectral efficiency than that of the time-domain counterpart [2,3]. Signal can also be additionally encoded in time domain (using two-dimensional (2-D) codes) so that even more users can be supported [3]. Furthermore, MW-OCDMA is especially favorable in the access network environment, as it does not require an expensive coherent source [4].

For design and deployment of MW-OCDMA in access networks, it is necessary to investigate the effects of physical layer impairments on the performance of MW-OCDMA-based systems. Though there have been many works devoted to this endeavor, including system performance analysis considering various noise, interferences such as receiver noise, multiple access interference (MAI), optical beating interference (OBI), and dispersion [5–12], the impact of four wave mixing (FWM), a nonlinear effect related to multi-wavelength transmission, has not been considered.

1.1 FWM in MW-OCDMA systems

Four-wave mixing (FWM) is a nonlinear phenomenon originating from the third order nonlinear susceptibility of optical fiber. Whenever three waves, assuming with frequencies of f_p, f_q and f_r, respectively ($r \neq p, q$), co-propagate inside the fiber and are overlapped in time,

#120788 - $15.00 USD Received 1 Dec 2009; revised 1 Mar 2010; accepted 22 Apr 2010; published 27 Apr 2010

they interact with each other through the third order nonlinear susceptibility of the optical fiber and generate a new wave at the frequency $f_i = f_p + f_q - f_r$ [13].

FWM is a well-studied issue in multi-wavelength optical networks, e.g. WDMA networks, with many studies devoted to the analysis of the impact of FWM on the system performance [13–17]. It is seen that FWM results in performance degradation [14,15] and its impact becomes especially critical when the number of wavelengths is large and/or the launched power is high [16].

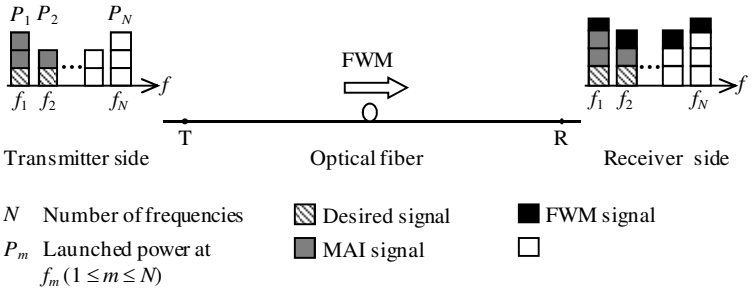

Fig. 1. Impact of FWM in MW-OCDMA systems

Considering Fig. 1, for a MW-OCDMA system using N frequencies, p, q, and r can vary from 1 to N resulting in a very large combination of new frequencies generated by FWM. In the case that existing frequencies are equally spaced, the new frequencies coincide with the existing ones, leading to crosstalk that causes incorrectness in the decoding process. Furthermore, the launched power at each frequency is relatively high because it is the total transmitted power from all users. FWM is therefore potentially a serious performance degradation factor in MW-OCDMA systems and hence should be well understood.

It is necessary to note that as each user in MW-OCDMA systems is allocated a set of multiple frequencies according to its signature code, the FWM power depends on not only conventional parameters such as the launched power and the number of frequencies, but also the parameters of signature code set. Combined with the decoding process at the receiving end, the impact of FWM on the performance of MW-OCDMA systems becomes more complex than that of wavelength-independent systems, such as WDM.

1.2 Main contributions

This paper, which is comprehensively extended from our previous works [18,19], presents the first quantitative analysis and detailed discussion on the FWM impairment in MW-OCDMA systems. In addition, many other interferences and noises including MAI, OBI, and receiver noise are also included in the analysis. The impact of FWM on various aspects of MW-OCDMA system performance such as bit-error rate (BER), number of users, and power penalty, is quantitatively discussed. To obtain the useful information for practical system design, we investigate the system performance with several types of optical fibers, including single mode fiber (SMF), dispersion-shifted fiber (DSF), and non-zero DSF (NZ-DSF). In addition, different values of frequency spacing are taken into account.

The rest of the paper is organized as follows. Section 2 presents the descriptions of the MW-OCDMA systems. FWM impact model is the content of Section 3. The performance analysis and numerical results are presented in Section 4 and 5, respectively. Finally, Section 6 concludes the paper.

#120788 - $15.00 USD Received 1 Dec 2009; revised 1 Mar 2010; accepted 22 Apr 2010; published 27 Apr 2010

2. System descriptions

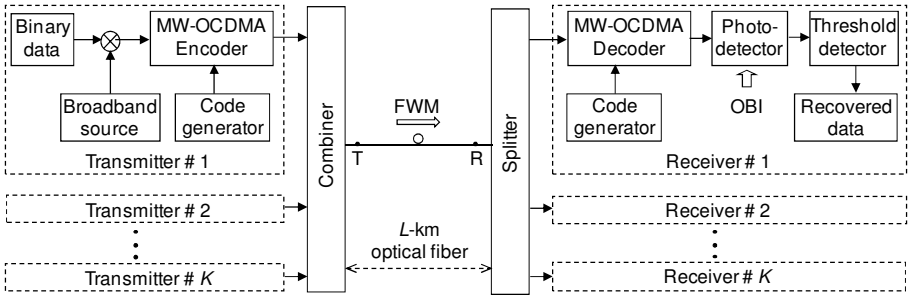

Fig. 2. Schematic diagram of a MW-OCDMA system.

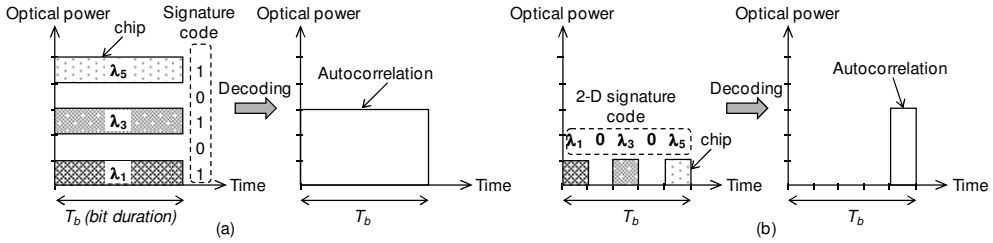

Fig. 3. Encoded signal and autocorrelation in the case of (a) 1-D spectral amplitude encoding and (b) 2-D encoding.

Figure 2 shows the schematic diagram of a MW-OCDMA system with K users. A set of a combiner and a splitter is used to combine the signals from all transmitters and broadcast them to all receivers. For illustrative purposes, one transmitter and one receiver are depicted in detail in this figure.

At the transmitter, an optical pulse coming from a broadband light source, whose spectrum is assumed flat, is first on-off keying (OOK) modulated by binary data. In OOK systems, an optical pulse is transmitted when a data bit is "1", otherwise no pulse is sent if the data bit is "0". The optical pulse corresponding to the data bit "1" is fed into a MW-OCDMA encoder, which can be implemented using the well-studied fiber Bragg gratings (FBGs) array structure [20,21].

In case of 1-D encoding, or spectral amplitude encoding (SAE), frequency components of optical pulse representing a bit "1" are selectively reflected at different FBGs, where each FBG is centered at a frequency (wavelength) defined by the corresponding signature code. More specifically, only frequency components corresponding to chip "1s" of the signature code can pass through the MW-OCDMA encoder. In case of 2-D encoding, reflected frequency components are additionally time-delayed in accordance with the second dimension of the signature code. In the FBG-based encoder, the time-delays are determined by the positions of FBGs in the array. The encoded signal in the case of 1-D and 2-D encoding are illustrated in Fig. 3(a) and Fig. 3(b), respectively.

The encoded signal is then combined with signals from other transmitters, transmitted over an optical fiber, and broadcasted to all receivers. When the multi-wavelength signal propagates along the optical fiber, FWM light is generated due to the interaction among the signals, which are overlapped in time but at different frequencies.

At the receiver, the received signal is first decoded by a MW-OCDMA decoder, which is also constructed by a FBGs array. In case of 1-D decoding, the desired signal from the targeted transmitter, whose frequencies are matched to FBGs tuned in the decoder, will be collected. The decoding process in case of 2-D also requires the frequency-matched pulses to be temporally coincided with the positions of the decoder's FBGs. For the receiver to decode signal from a specific transmitter, its FBGs are tuned to the same frequencies as those in the

#120788 - $15.00 USD Received 1 Dec 2009; revised 1 Mar 2010; accepted 22 Apr 2010; published 27 Apr 2010

transmitter. Additionally in case of 2-D decoding, the positions of FBGs are in the inverse order of those in the transmitter [10].

The output of the decoder consists of an autocorrelation peak of height w (w is the code weight of the signature code) as shown in Fig. 3. MAI and FWM light, whose frequencies are coincided to desired ones, affect on the autocorrelation peak and may cause bit error. Decoded signal is then converted into photocurrent by a photodetector (PD). It is at the PD, OBI will occur due to the beating between signals with nearly the same frequency. Finally, the binary data is recovered by a threshold detector.

3. FWM impact model

Through FWM process, three waves of frequency f_p, f_q and f_r ($r \neq p, q$) interact and generate a new frequency $f_i = f_p + f_q - f_r$. The power of FWM light at frequency f_i can be expressed as [13]

$$P_{pqr} = \eta_F \left(d_F \gamma L\right)^2 \left(n_p P_c\right)\left(n_q P_c\right)\left(n_r P_c\right)\exp\left(-\alpha L\right), \tag{1}$$

where d_F is the degeneracy factor defined such that its value is 1 when $p = q$ but 2 when $p \neq q$. L is the transmission length, γ is the nonlinearity coefficient, and α is the attenuation coefficient of the optical fiber. P_c is the transmitted power per chip pulse (i.e. chip "1"), which is assumed to be the same for all users and frequencies. n_p, n_q, and n_r are the number of pulses appearing at the frequencies f_p, f_q, and f_r in one chip period ($1 \le p, q, r \le N$). $n_p P_c$, $n_q P_c$ and $n_r P_c$ are therefore the launched power (i.e. the power at T-point in Fig. 2) at the frequencies f_p, f_q, and f_r, respectively. η_F is the FWM efficiency defined as [13]

$$\eta_F = \left|\frac{1-\exp\left[-\left(\alpha + j\Delta k\right)L\right]}{\left(\alpha + j\Delta k\right)L}\right|^2. \tag{2}$$

The FWM efficiency η_F depends on the frequency spacing through the phase match governed by

$$\Delta k \approx \beta_2 \left(\omega_p - \omega_r\right)\left(\omega_q - \omega_r\right), \tag{3}$$

where β_2 is the group velocity dispersion parameter at $\omega_c = (\omega_p + \omega_q)/2$ ($\omega_{p,q,r} = 2\pi f_{p,q,r}$).

As mentioned in Section 1.1, when p, q, and r vary from 1 to N, there are different combinations of f_p, f_q, and f_r that generate the frequencies coinciding with the existing ones. For example, in a system with four equally spaced frequencies (N = 4; f_1, f_2, f_3 and f_4), the number of combinations generating FWM light at the frequency f_1 or f_4 is three, while it is five at the frequency f_2 or f_3, as shown in Table 1.

Table 1. Frequency combinations caused by FWM in a 4-equally-spaced frequency system (N = 4)

Existing frequency	f_1	$f_2 = f_1 + \Delta f$	$f_3 = f_1 + 2\Delta f$	$f_4 = f_1 + 3\Delta f$
Frequency combination	$f_1 = f_2 + f_2 - f_3$	$f_2 = f_1 + f_3 - f_2$	$f_3 = f_1 + f_4 - f_2$	$f_4 = f_2 + f_3 - f_1$
	$f_1 = f_2 + f_3 - f_4$	$f_2 = f_3 + f_1 - f_2$	$f_3 = f_4 + f_1 - f_2$	$f_4 = f_3 + f_2 - f_1$
	$f_1 = f_3 + f_2 - f_4$	$f_2 = f_1 + f_4 - f_3$	$f_3 = f_2 + f_4 - f_3$	$f_4 = f_3 + f_3 - f_2$
		$f_2 = f_4 + f_1 - f_3$	$f_3 = f_4 + f_2 - f_3$	
		$f_2 = f_3 + f_3 - f_4$	$f_3 = f_2 + f_2 - f_4$	

Denote P_i^F as the total power of FWM light generated at frequency f_i, it can be calculated as

$$P_i^F = \sum_{pqr} P_{pqr}, \tag{4}$$

#120788 - $15.00 USD Received 1 Dec 2009; revised 1 Mar 2010; accepted 22 Apr 2010; published 27 Apr 2010

where the summation term in Eq. (4) contains all combinations satisfying the condition $f_p + f_q - f_r = f_i$. The power of each combination (P_{pqr}) is obtained from Eq. (1).

4. Performance analysis

In this section, we will theoretically analyze the performance of MW-OCDMA systems based on the FWM impact model discussed in Section 3. We consider both types of MW-OCDMA systems, including 1-D encoding (SAE) [2] and 2-D encoding OCDMA systems, in which transmitted signals are encoded using both frequency and time domains [3]. Besides the impact of FWM, we also take into account MAI, OBI, and receiver noise. In order to focus on the impact of FWM, the group velocity dispersion (GVD), self-phase mixing, and cross-phase mixing on the system performance is neglected in the analysis. The discussion on the impact of GVD on 2-D OCDMA systems can be found in [11], and as a matter of fact, GVD can be effectively compensated by using DSF or GVD compensation techniques [12,22].

In the following analysis, we assume that the bit and chip streams from all users are to be synchronized, i.e., the worst performance since the FWM-induced power is the strongest in this case. The binary channel is also assumed equally likely, i.e. the probabilities that a transmitter sends bit "1" and bit "0" are the same and equal to 1/2. In addition, we denote w as the number of frequencies assigned to each user, which is also the code weight of the signature code. Without loss of generality, the w frequencies for targeted transmitter (desired frequencies) are denoted from 1 to w. The remaining ones (i.e., N - w frequencies) are considered as undesired frequencies and denoted from w + 1 to N.

4.1 BER in SAE/OCDMA systems

In SAE/OCDMA systems, a receiver structure with two decoders connecting in a balance fashion, as shown in the Fig. 4, is employed so that MAI can be completely removed [2]. The desired frequencies are collected by the direct decoder while the undesired ones will pass through the complementary decoder. To completely cancel MAI, a ratio between the optical powers that arrive at the two photodetectors is set to $\xi = \lambda/(w - \lambda)$, where λ is the cross-correlation value of the signature code [9].

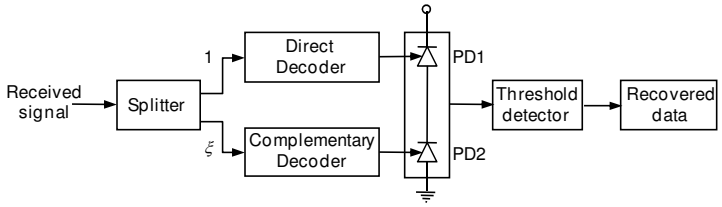

Fig. 4. Receiver structure of a SAE/OCDMA system.

When a transmitter sends bit "1", its w pulses are visible at w frequencies, i.e., one at each frequency. The probability that a pulse appears at a specific frequency can be expressed as $p_m = w/N$. Consider a whole system with K users, the total number of pulses at a specific frequency (n_p, n_q, or n_r) can be modeled as a binomial random variable with a probability $p_m/2$ (the probability of sending bit "1" is 1/2). According to the property of the signature code set, when the number of users is large enough, optical pulses from all transmitters are equally distributed over N frequencies. As a result, we can estimate n_p, n_q, and n_r using averaging approach and the product of n_p, n_q, and n_r in the calculation of FWM light [Eq. (1)] can be replaced with $(K p_m/2)^3$.

As the impact of GVD is ignored, MAI current is completely eliminated in SAE/OCDMA systems [3]. The total signal current at the output of the balanced detector considering FWM impact therefore can be derived as

#120788 - $15.00 USD Received 1 Dec 2009; revised 1 Mar 2010; accepted 22 Apr 2010; published 27 Apr 2010

$$I_b^{(SAE)} = \Re\left(\underbrace{bwP_s}_{\substack{\text{desired}\\ \text{signal}}} + \underbrace{\sum_{i=1}^{w} P_i^F - \sum_{i=w+1}^{N} \xi P_i^F}_{\text{FWM light}}\right), \tag{5}$$

where $b = 1$ (or 0) when the targeted transmitter sends bit "1" (or bit "0"). $\Re$ is denoted as the PD responsivity and P_s is the received power per chip pulse. The relation between P_s and P_c is $P_s = [P_c \exp(-\alpha L)]/K$. Note that the FWM-induced current is contributed from FWM light at both w desired frequencies and $(N - w)$ undesired ones.

Besides the OBI currents caused by the beating between desired and interfering pulses, and the beating among interfering pulses [7], when FWM is taken into consideration, additional OBI currents are generated. These OBI currents are caused by the beating between FWM light and desired, interfering pulses. The total variance of OBIs therefore can be calculated as

$$i_{OBI}^{2(SAE)} = 2B_e\tau_c\Re^2\left[\underbrace{P_s^2\sum_{i=1}^{w}\left(bk_i + \binom{k_i}{2}\right)}_{\text{MAI-induced OBI}} + \underbrace{P_s\sum_{i=1}^{w}(b+k_i)P_i^F}_{\text{FWM-induced OBI}} + \underbrace{(\xi P_s)^2\sum_{i=w+1}^{N}\binom{k_i}{2}}_{\text{MAI-induced OBI}} + \underbrace{\xi^2 P_s\sum_{i=w+1}^{N}k_i P_i^F}_{\text{FWM-induced OBI}}\right], \tag{6}$$

where B_e is the PD electrical bandwidth. τ_c is the coherent time of the broadband source, which can be approximated as $\tau_c = 1/B_0$, where B_0 is the optical bandwidth. k_i is the number of interfering pulses at the frequency f_i. The interfering pulses are from interfering users sending bit "1" denoted as k. The event k out of possible $K - 1$ interfering users sending bit "1" can be modeled as a binomial distribution with probability 1/2. When k is large enough, similarly, interfering pulses are equally distributed over N frequencies. As a result, the total variance of OBI can be calculated by replacing k_i in Eq. (6) with its average value $\langle k_i \rangle = 0.5(K-1)w/N$.

The receiver noise includes the contribution from both shot noise $i_s^2 = 2eB_eI_b$ and thermal noise $i_{th}^2 = 8\pi k_B T_n B_e^2 C$, where e is the electron charge, k_B is Boltzman's constant, T_n is the receiver noise temperature, and C is the receiver capacitance. The total noise variance, i_{nb}^2 ($b \in \{0,1\}$), is expressed as follows

$$i_{nb}^2 = i_{OBIb}^{2(SAE)} + i_{sb}^2 + i_{th}^2. \tag{7}$$

Each bit is detected by comparing the total signal current with a threshold current I_D. The photocurrent as well as noises and interferences can be modeled as Gaussian random variables and the total probability of error can be calculated as

$$\text{BER} = \frac{1}{2}\left[Q\left(\frac{I_1 - I_D}{i_{n1}}\right) + Q\left(\frac{I_D - I_0}{i_{n0}}\right)\right], \tag{8}$$

where I_1 and I_0 are the total signal current (I_b, $b = 1$ or 0) obtained from Eq. (5). Also, i_{n1} and i_{n0} are i_{nb} with $b = 1$ and $b = 0$. Q function is written by

$$Q(x) = \frac{1}{2\pi}\int_x^{\infty}\exp\left(-y^2/2\right)dy. \tag{9}$$

To minimize the BER, we consider the case that I_D is optimum [13], $I_D = (i_{n0}I_1 + i_{n1}I_0)/(i_{n0} + i_{n1})$. The total probability of error hence can be expressed as

$$\text{BER} = Q\left(\frac{I_1 - I_0}{i_{n1} + i_{n0}}\right). \tag{10}$$

#120788 - $15.00 USD Received 1 Dec 2009; revised 1 Mar 2010; accepted 22 Apr 2010; published 27 Apr 2010

4.2 BER in 2-D OCDMA systems

We now extend our discussion to 2-D OCDMA systems, whose 2-D signature codes consists of a time-spreading pattern and a wavelength-hopping pattern. Denote β as the maximum number of overlapping pulses between the time-spreading pattern of an interfering user and the desired one's, the probability that one interfering pulse belongs to a desired chip period (out of w ones) is β /w. Furthermore, this interfering pulse can be visible at one of N frequencies. As a result, the probability that one interfering pulse appears at one specific frequency in one specific chip period is calculated as $p_m = \beta /(wN)$. Using the same approach with SAE/OCDMA systems, we can estimate the FWM light in 2-D OCDMA systems.

In 2-D OCDMA systems, MAI current will appear in the total signal current. Denote k_i as the number of MAI pulses at frequency f_i, the total signal current hence can be expressed as

$$I_b^{(2-D)} = \Re\left(\underbrace{bwP_s}_{\substack{\text{desired}\\ \text{signal}}} + \underbrace{\sum_{i=1}^{w}\sum_{j=1}^{k_i} P_s}_{\text{MAI signal}} + \underbrace{\sum_{i=1}^{w} P_i^F}_{\text{FWM light}} \right). \tag{11}$$

As only signal at w desired frequencies can pass through the decoder, the total variance of OBIs is thus derived as

$$i_{OBIb}^{2(2-D)} = 2B_e\tau_c\Re^2\left[\underbrace{P_s^2\sum_{i=1}^{w}\left(bk_i + \binom{k_i}{2} \right)}_{\text{MAI-induced OBI}} + \underbrace{P_s\sum_{i=1}^{w}\left(b+k_i\right)P_i^F}_{\text{FWM-induced OBI}} \right]. \tag{12}$$

To calculate the total signal current and OBI, the number of MAI pulses at each frequency (i.e., k_i) needs to be obtained. Defining p_{MAI} as the probability that one pulse from an interfering user matches with a desired one in both time and frequency (i.e., MAI pulse), p_{MAI} depends on the signature code set and will be mentioned in detail in the numerical result section. The event that there are j MAI pulses generated from k interfering users sending bit "1" can also be modeled as a binomial distribution with probability p_{MAI}. When the number of interfering users is large enough, MAI pulses can be assumed to be equally distributed over w desired frequencies, k_i hence can be replaced by its average value $\langle k_i \rangle = j/w$.

The receiver noise as well as the total noise variance is calculated in a similar way with SAE/OCDMA system. As a result, the total probability of error can be calculated as [7]

$$\text{BER} = \sum_{k=1}^{K-1}\binom{K-1}{k} 2^{-(K-1)} \sum_{j=1}^{k}\binom{k}{j} p_{\text{MAI}}^{j}\left(1-p_{\text{MAI}}\right)^{k-j} Q\left(\frac{I_1 - I_0}{i_{n1}+i_{n0}}\right). \tag{13}$$

5. Numerical results

In our analysis, the N frequencies used in the system are centered at 193.4 GHz, which corresponds to the wavelength 1550.12 nm. The frequency spacing is chosen as 25 GHz, 50 GHz, and 100 GHz in accordance with standard ITU for DWDM [23]. As the OCDMA is proposed for broadband optical access networks, we are interested in the system that can support at least 32 users with bit rate of 1Gbit/s per user. Other system parameters and constants used in the analysis are shown in Table 2.

#120788 - $15.00 USD Received 1 Dec 2009; revised 1 Mar 2010; accepted 22 Apr 2010; published 27 Apr 2010

Table 2. System parameters and constants

Name	*Symbol*	*Value*
Boltzmann's constant	k_B	1.38×10^{-23} W/K/Hz
Electron charge	E	1.6×10^{-19} C
Light velocity	C	3×10^{8} m/s
Receiver capacitance	C	0.02×10^{-12} F
Noise temperature	T_n	300 K
PD responsivity	$\Re$	1 A/W
Bit rate per user	B_e	1 Gbit/s

In addition, three types of optical fiber are considered in this analysis including normal SMF [24], DSF [25], and NZ-DSF [26] with attenuation coefficient α = 0.2 dB/km at wavelength 1550 nm. The dispersion coefficient D, the dispersion slope coefficient S, and the nonlinear parameter γ of optical fibers are shown in Table 3.

Table 3. Optical fiber parameters

Fiber	D (ps/nm × km)	S (ps/nm^2 × km)	γ (W^{-1}/km)
SMF	16	0.08	1.3
DSF	1	0.08	3
NZ-DSF	4	0.08	1.46

5.1 SAE/OCDMA systems

Several signature code sets can be used in SAE/OCDMA systems, including m-sequence, Hadamard, and modified quadratic congruence (MQC) code [2,6,8]. Of these codes, MQC offers the best performance when OBI is considered [8]. In fact, it is not practical to use m-sequence, Hadamard codes in the considered system, which is expected to support at least 32 users with bit rate per user of 1 Gbit/s [9]. In the following discussion, we therefore consider only SAE/OCDMA systems using MQC code.

MQC codes are defined by an odd prime number p. The code weight and the code length are $w = p + 1$ and $N = p^2 + p$, respectively. The cross-correlation is one and the cardinality of a MQC code set is p^2. For the system to support 32 × 1 Gbit/s users with adequate BER, MQC code with $p = 11$ is used, equivalently we have $(N, w, \lambda) = (132, 12, 1)$.

We first investigate the BER versus transmitted power per chip P_c when K = 32 users, the transmission length L = 30 km. Figure 5 shows that the transmitted power range can be divided into two regions: receiver noise-dominant and FWM-dominant regions. In the first one, the BER decreases when P_c is increased. However, reverse phenomenon occurs in the second region. This is because FWM power strongly increases when P_c is large enough and its impact becomes dominant compared with the receiver noise. At the threshold power, i.e., the boundary between two regions, BER reaches the smallest value. For example, the threshold power is −12 dBm for the case of using SMF.

#120788 - $15.00 USD Received 1 Dec 2009; revised 1 Mar 2010; accepted 22 Apr 2010; published 27 Apr 2010

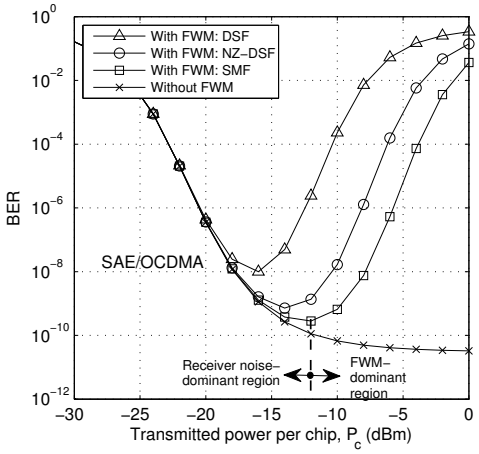

Fig. 5. BER versus the transmitted power per chip with different types of fibers when K = 32 users, L = 30 km, Δf = 25 GHz, and MQC code set is used.

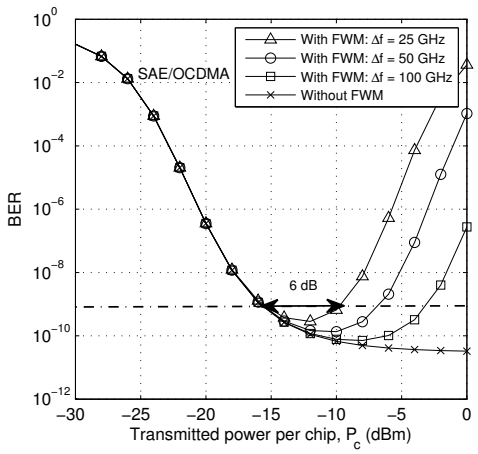

Fig. 6. BER versus the transmitted power per chip with different frequency spacing when K = 32 users and L = 30 km. MQC code set and SMF are used.

In addition, in Fig. 5, the performance of the SAE/OCDMA system using different types of optical fibers is shown. It is seen that, as the nonlinear parameter of SMF is smaller, the system using SMF is less affected by FWM than the one using NZ-DSF or DSF. More specifically, at P_c = −12 dBm, the power penalty is 2.2 dB for the system using SMF whereas it is 4.1 dB and 9 dB for the one using NZ-DSF and DSF, respectively.

Next, the relation between the BER and the transmitted power per chip P_c is investigated with different frequency spacing. The system performance with three values of frequency spacing, including 25 GHz, 50 GHz, and 100 GHz, is shown in Fig. 6. It is seen that when the frequency spacing is increased, the operational power range, the range at which BER ≤ 10^{-9} can be maintained, is extended. As shown in the figure, it is extended from 6 dB to 12.7 dB when frequency spacing is increased from 25 GHz to 100 GHz.

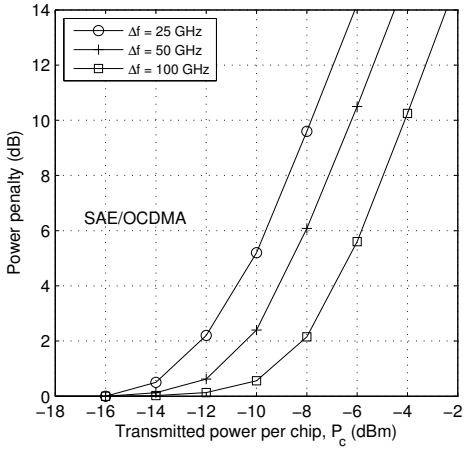

Fig. 7. Power penalty versus the transmitted power per chip in the case of using SMF and MQC code set when K = 32 users and L = 30 km.

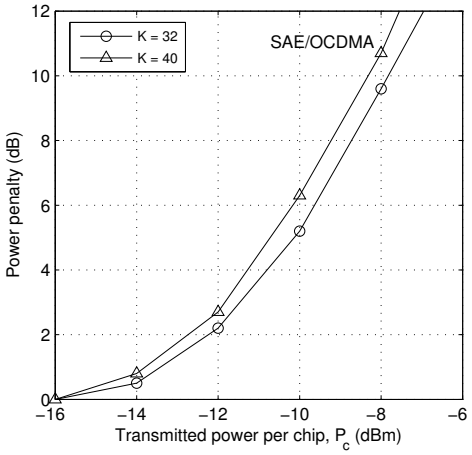

Fig. 8. Power penalty versus the transmitted power per chip when L = 30 km, Δf = 25 GHz, and SMF is used.

#120788 - $15.00 USD Received 1 Dec 2009; revised 1 Mar 2010; accepted 22 Apr 2010; published 27 Apr 2010

The influence of frequency spacing is further investigated in Fig. 7 when the power penalty versus transmitted power per chip is shown. The number of active users is 32, the transmission length is also 30 km. Similarly, the increase of frequency spacing helps to reduce the power penalty. Additionally, it is seen that the power penalty due to the impact of FWM is significantly high when the optical power per chip is high, especially for the case of narrow frequency spacing, for example, 9.6 dB for the case that frequency spacing is 25 GHz at P_c = −8 dBm.

Finally, in Fig. 8, we investigate power penalty versus the transmitted power per chip when K = 32 and 40 users. It is found that the higher K results in the higher power penalty under the impact of FWM. This is because, when there are more users, the total launch power at a wavelength becomes higher, which consequently results in higher FMW.

5.2 2-D OCDMA systems

In this paper, we consider the 2-D OCDMA systems using 2-D signature codes constructed by the popular prime sequences. The 2-D signature code set based on prime sequences is characterized by two prime numbers, p_s and p_h ($p_h \geq p_s$), which are used, respectively, for generating time-spreading and wavelength-hopping patterns. This 2-D signature code has weight of p_s (i.e., $w = p_s$); and p_h is the number of available frequencies in the system (i.e., $N = p_h$). The cardinality of the 2-D prime code set is $p_s \times (p_h - 1)$. The details about structure and properties of 2-D signature codes can be found in [4]. When this 2-D signature codes are used, the probability p_{MAI} in corresponding to a pair of p_s and p_h then can be expressed as $p_{\mathrm{MAI}} = \mu_\lambda / p_s^2$ [7], where

$$\mu_\lambda = \frac{1}{\binom{p_h}{p_s}} \left\{ \binom{p_h - 1}{p_s - 1} \frac{(p_s - 1)(p_s - 2) + (p_h - 2)}{p_h - 2} + \binom{p_h - 1}{p_s} \frac{p_s (p_s - 1)}{p_h - 2} \right\} \qquad (14)$$

is the average number of wavelengths common to a pair of two prime signature code.

We are interested in finding the operational range of transmitted power per chip. Due to the nature of the 2-D signature code based on prime sequence, the minimum and maximum operation ranges can be found in two special cases: (1) all users have the same time spreading pattern, and (2) all users have different time spreading patterns. Accordingly, we have $\beta = p_s$ for the first case, and $\beta = 2$ for the second one [4].

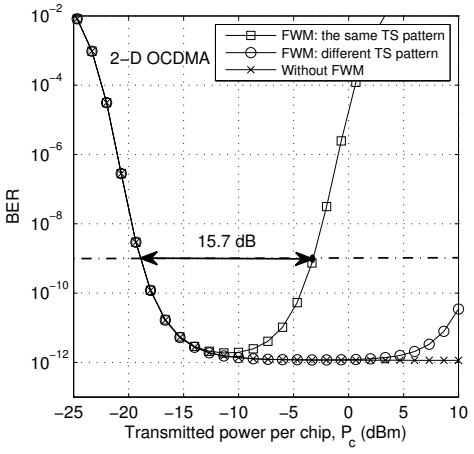

Fig. 9. BER versus the transmitted power per chip in the case of using SMF when K = 32 users, L = 60 km, and Δf = 25 GHz.

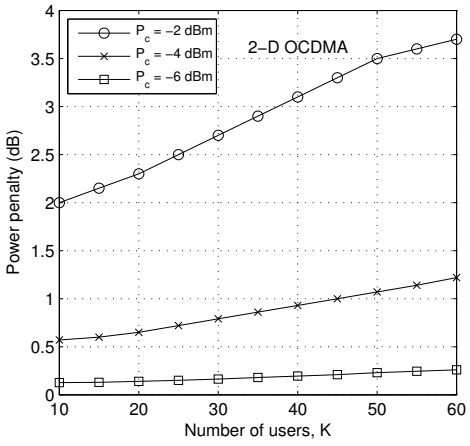

Fig. 10. Power penalty versus the number of users in the case of using SMF when L = 60 km and Δf = 25 GHz.

#120788 - $15.00 USD Received 1 Dec 2009; revised 1 Mar 2010; accepted 22 Apr 2010; published 27 Apr 2010

Figure 9 shows BER versus the transmitted power per chip when $p_s = 29$ and $p_h = 31$. The frequency spacing is 25 GHz and the transmission length is 60 km. The number of active users is 30. The operational range of the transmitted power per chip is the most narrow when all users use the same time-spreading pattern and it is about 15.7 dB. On the other hand, this range is extended in the case that different patterns are used.

Finally, we assume all users use different time-spreading patterns and investigate the power penalty when the number of active users increases. Several values of the transmitted power per chip, $P_c = -6$, -4, and -2 dBm, are used with the frequency spacing is 25 GHz and the transmission length is 60 km. Figure 10 shows that the power penalty increases in proportion with the number of users, especially when the transmitted power per chip is high. Specifically, the power penalty is almost 0.5 dB for every ten-user more when the transmitted power per chip is −2 dBm.

6. Conclusion

We have theoretically analyzed the impact of FWM on the performance of MW-OCDMA systems considering many other noises and interferences. We presented a quantitative discussion about the impact of FWM on various aspects of MW-OCDMA system performance, including the BER, the number of users, and the power penalty. We also investigated the system performance with several types of optical fibers such as SMF, DSF, and NZ-DSF taking account different values of frequency spacing. The numerical results show that FWM causes an increase in the BER of the systems, especially when transmitted power is high, frequency spacing is small, or DSF is used. FWM also limit the operational power range of the system. For example, it is only 6 dB in the case of SAE/OCDMA system using MQC code of (132, 12, 1). In addition, the impact of FWM is quantified by power penalty and investigated with different number of users to provide useful information for practical system design.

Acknowledgments

The authors thank the reviewers for their thorough reviews and useful suggestions for improving the readability of this paper. This work was supported in part by the Japan Society for the Promotion of Science under Grants-in-Aid No. 18760278.

#120788 - $15.00 USD Received 1 Dec 2009; revised 1 Mar 2010; accepted 22 Apr 2010; published 27 Apr 2010